BULLETIN OF THE POLISH ACADEMY OF SCIENCES
TECHNICAL SCIENCES
DOI: 10.24425/bpasts.2026.158771

Design and rapid levelling control strategy of omnidirectional levelling system for tractor seat in hilly and mountainous terrain

Chen Li[1] , Junjiang Zhang[1, 2, 3, *] , Shuaishuai Ge[2] , Mengnan Liu[1, 3] , Liyou Xu[1, 3,] and Xianghai Yan[1, 3]

[1] College of Vehicle and Traffic Engineering, Henan University of Science and Technology, Luoyang, 471003, China
[2] China Key Laboratory of Advanced Manufacture Technology for Automobile Parts (Chongqing University of Technology), Ministry of Education
[3] YTO Group Corporation, Luoyang, 471004, China

Abstract. To address the problem of reduced comfort caused by vehicle tilt for hilly tractor driver, a novel seat posture omnidirectional levelling system is designed, and an omnidirectional rapid levelling control strategy (QBP-PID) is proposed, which fuses Q-learning, Back Propagation (BP) neural network, and Proportional-Integral-Derivative (PID) control. Firstly, an omnidirectional levelling system for seat posture is designed based on kinematic principles. On this basis, a model for the omnidirectional levelling system is established using valve-controlled hydraulic cylinder principles. Subsequently, addressing the challenge of difficult parameter tuning for the levelling system's PID control, a multi-level parameter update strategy employing QBP-PID is proposed for rapid omnidirectional levelling control. Simulation results show that under QBP-PID control, the 15° lateral levelling time is 2.98 s with an overshoot of 0.32°; The longitudinal levelling time at 20° is 3.41 s with an overshoot of 0.95°. Compared to BP-PID and PID, the lateral levelling time is reduced by 18.13% and 27.66% respectively, while the longitudinal levelling time decreased by 17.63% and 31.6% respectively. The superiority of the QBP-PID omnidirectional rapid levelling control strategy has been demonstrated.

Key words: seat posture, omnidirectional levelling, back propagation neural network, Q-learning.

1. INTRODUCTION

Hilly and mountainous terrain accounts for approximately 24% of the world's land area, extending across multiple continents including Asia, Europe and the Americas. It constitutes one of the key regions for agricultural production [1]. However, the rugged terrain, steep slopes and narrow roads in such areas pose significant challenges to agricultural mechanization operations [2-4]. As the primary power source for agricultural production in hilly and mountainous terrain, the performance of tractor directly impacts the quality of field operations [5-8]. In response to the issue of reduced driver comfort arising from altered seating positions due to cab tilt during ploughing operations on hilly terrain with varying ridge heights, levelling technology emerges as a critical solution. This technology effectively enhances the driver's experience and boosts operational efficiency [9,10]. With the continuous advancement of intelligent and automated technologies, related research has garnered increasing attention.

Levelling systems were first applied to the body levelling of agricultural machinery. Tracked combine harvesters produced by Japanese companies such as Kubota and Daido utilize track lifting mechanisms to adjust the height of individual tracks, thereby compensating for lateral body tilt [11,12]. In the paper [13], a manually operated levelling mechanism for mowers was devised to ensure the cutting deck remains consistently level with the tractor. In the paper [14], a levelling system for combine harvester header was devised. However, the above levelling systems are not suitable for certain working conditions, such as mountainous tractor ploughing operations. In the paper [15], an automatic tractor body levelling system was devised that controls the extension and retraction of hydraulic cylinders by acquiring tilt information from the tractor body, thereby adjusting the tractor's posture. In the papers [16,17], an adaptive levelling chassis suitable for hilly terrain was designed, reducing chassis roll and pitch angles through dynamic levelling. In the paper [18], a posture adjustment mechanism based on a parallel four-bar linkage was proposed, enabling lateral and longitudinal posture adjustments of the body. Regarding cab levelling technology, the SKH-60 mountain tractor produced by Swiss company Rigi and the Terratrac series mountain tractors manufactured by Swiss firm Aebi feature adjustable cab posture functionality [8]. Regarding driving comfort enhancements, while body and cab levelling improve overall machine stability, these systems suffer from

*e-mail: zhangjunjiang2020@163.com

high adjustment masses, slow response times, and potential impacts on vehicle centre of gravity distribution and handling characteristics. Seat levelling technology, however, offers advantages of low adjustment mass and rapid response, enabling precise real-time compensation. As an independent system, it causes minimal interference with the vehicle as a whole and offers high safety. However, seat levelling primarily addresses perceived seating posture without eliminating visual inclination, and its adjustment range is structurally constrained. After comprehensively weighing performance, cost, safety, and engineering feasibility, seat levelling technology is deemed the most cost-effective and viable solution for enhancing driving comfort in hilly terrain tractors under current technical conditions. As regards seat posture levelling systems, their practical application to tractor seat remains relatively uncommon, with most tractor seat levelling research and development still largely confined to the prototype development stage. In the paper [19], an automatic levelling system for agricultural machinery driver seat was investigated, achieving lateral levelling between 2° and 13°. In the paper [20], a seat levelling device capable of automatically adjusting the driver's seat according to the machine's lateral tilt angle during operation was designed. In the paper [21], a seat cushion levelling device was developed and field trials were conducted on the Dongfanghong LX754 tractor, verifying its practicality. However, the above studies focused solely on lateral levelling, failing to address the driver's forward or backward leaning caused by pitch attitude changes when the machinery traverses slopes or encounters undulating terrain. Consequently, achieving omnidirectional seat levelling is crucial for ensuring sustained driving comfort and operational stability.

To achieve precise and rapid response in a seat levelling system, mechanical design alone is insufficient; efficient and intelligent control methods play a decisive role. Currently, Proportional-Integral-Derivative (PID) control is predominantly employed for levelling systems, with common variants including classical PID control, fuzzy PID control, dual-loop fuzzy PID control, and PID control based on back propagation neural network (BP-PID). In the paper [22], an automatic levelling system for rotary tillers was designed, employing a PID controller to regulate the electromagnetic directional control valve and thereby control hydraulic cylinder operation for automatic implement levelling. However, the PID parameter tuning process proved complex, yielding suboptimal control performance. In the paper [23], a fuzzy PID control algorithm for a tractor automatic levelling control system was developed, establishing mathematical models for X-axis and Y-axis velocity levelling control of the tractor chassis platform. In the paper [24], a dual-closed-loop fuzzy PID control algorithm was devised capable of proactively adjusting the tractor chassis's posture according to terrain characteristics, demonstrating favorable adaptability on slopes. Whilst the fuzzy PID approach achieves adaptive parameter tuning, its fuzzy rules rely on expert knowledge and lack self-learning capabilities. In the paper [25], a synchronous control system for vehicle body and agricultural implement posture based on a neural network PID algorithm was designed, enhancing the response speed and control accuracy of the posture control system. In the paper [26], a neural network PID control algorithm for vehicle chassis automatic levelling control systems was proposed, addressing issues of overshoot and high levelling delay in PID control. However, neural networks are prone to local optima and their training convergence requires improvement. In addition, in the paper [27], reinforcement-learning (RL)-based adaptive PID control strategies have recently been reported. Although such approaches exhibit strong self-learning capability, they typically enlarge the action space and increase computational burden, which may limit their real-time applicability in electro-hydraulic systems. In recent years, model-free Q-learning algorithms with autonomous learning capabilities have demonstrated significant potential in complex system control [28,29]. Integrating these with neural networks holds promise for overcoming limitations in existing control strategies and achieving higher-precision adaptive control. Compared with existing hybrid control methods based on neural networks and reinforcement learning, the proposed QBP-PID strategy presents a distinct structural characteristic. In conventional BP-PID, PID parameters are updated solely via gradient descent, which may lead to slow convergence and local optima. In RL-based adaptive PID, reinforcement learning directly adjusts controller parameters or actions, increasing computational complexity. In contrast, the proposed approach employs Q-learning to optimize the BP weight update dynamics rather than directly acting on the hydraulic system. This results in a hierarchical and lightweight hybrid structure that preserves PID interpretability and stability while improving convergence and adaptability. However, research applying this advanced composite control algorithm to address real-time seat posture levelling for tractor in hilly and mountainous terrain remains unexplored. A comparison of adaptive PID-based control is summarized in Table 1.

TABLE 1. Comparison of adaptive PID-based control strategies

Control strategy	Parameter adaptation	Self-learning ability	Computational complexity	Real-Time Suitability
Classical PID	Manual tuning	None	Low	High
Fuzzy PID	Rule-based adjustment	Limited	Medium	Moderate
BP-PID	Neural network tuning	Yes	Medium	Moderate
RL-based PID	Direct RL adjustment of gains/actions	Strong	High	Moderate–Low
Proposed QBP-PID	BP tuning + Q-learning dynamics	Strong	Moderate	High

It should be noted that, unlike RL-based PID methods where reinforcement learning directly optimizes controller actions or parameters, the proposed QBP-PID strategy only uses Q-learning to adjust the momentum factor in the BP neural

network weight update process. Therefore, the action space remains small and the online computational burden is reduced.

Based on this, this paper addresses the requirement for seat posture levelling in tractor operating in hilly and mountainous terrain. Utilizing principles of kinematics, a novel seat posture omnidirectional levelling system is designed. Building upon this, a model for the seat posture omnidirectional levelling system is established based on valve-controlled hydraulic cylinder principles, and a QBP-PID omnidirectional rapid levelling control strategy is proposed, which fuses Q-learning, back propagation neural network, and PID control. The core of this paper is to achieve omnidirectional, rapid and precise levelling of the seat's posture, thereby enhancing driver comfort and safety during slope operations and advancing the intelligent development of agricultural machinery for hilly and mountainous terrain. The main innovations of this paper are as follows:

(1) Addressing driving comfort issues for tractor operators in hilly and mountainous terrain caused by vehicle tilt, a novel seat posture omnidirectional levelling system is designed based on kinematic principles.
(2) To overcome the difficulty in tuning PID control parameters for the omnidirectional seat levelling system, a QBP-PID rapid levelling control strategy integrating Q-learning, BP neural network and PID control is proposed.

The rest of this paper are as follows: Section 2 details the design of the novel omnidirectional seat posture levelling system. The novel seat posture omnidirectional levelling system is designed in Section 3. Section 4 proposes the QBP-PID rapid levelling control strategy. Section 5 presents simulation analyses. Section 6 summarizes the main conclusions of this paper.

2. DESIGN OF THE SEAT POSTURE OMNIDIRECTIONAL LEVELLING SYSTEM

The core of the seat posture levelling system lies in its posture adjustment actuator. Conventional seat levelling systems can only adjust the seat's lateral tilt angle. When operating on complex terrain, such as hilly or mountainous regions, where the tractor undergoes pitching motions, maintaining the driver's comfortable seating position becomes challenging. To address this limitation, a novel seat posture omnidirectional levelling system is designed in this paper. Its innovation lies in achieving posture levelling across both lateral and longitudinal degrees of freedom, thereby realizing true omnidirectional levelling. Section 2.1 first designs the seat posture omnidirectional levelling system based on kinematic principles, establishing the relationship between hydraulic cylinder displacement and seat tilt angle. Subsequently, Section 2.2 outlines the operational principles of the seat posture omnidirectional levelling system and details the design of its hydraulic circuit.

2.1. The seat posture omnidirectional levelling system

To address the complex terrain of hills and mountains with steep slopes and narrow roads, this paper employs seat posture levelling technology to enhance driver comfort. Capitalizing on the characteristic that the longitudinal installation space of the seat exceeds its lateral dimensions, the designed levelling system achieves a greater longitudinal levelling angle. The omnidirectional levelling system designed in this paper is essentially a simplified configuration of the Stewart platform. As a classic parallel structure, the Stewart platform offers advantages such as compact design, high rigidity, and high motion precision. Its stability has been extensively validated in the field of multi-degree-of-freedom attitude control. The structure of the novel seat posture omnidirectional levelling system is illustrated in Fig. 1, comprising three components: the seat, the seat suspension, and the levelling system. The seat posture omnidirectional levelling system serves as the core actuator for achieving full-range seat posture adjustment in hill-terrain tractors. The overall seat posture levelling system configuration comprises: an upper layer forming the seat plane; a middle layer comprising the seat suspension, which includes a scissor-type seat structure, coil spring, and damper. The elastic element is a coil spring. The two shear arms are connected to each other, and the connection between the shear arms and the upper/lower base plates forms a hinge mechanism. The lower layer comprises the omnidirectional levelling system, which connects to the middle layer suspension base and the lower levelling base via hydraulic cylinders. The seat plane, seat suspension, and omnidirectional levelling system form a three-layer structure. This design reduces the working load on the hydraulic cylinders and enhances the system's load-bearing capacity. The intermediate suspension base and lower levelling base employ a separate hydraulic system. Through the extension and compression of hydraulic cylinders, the seat maintains horizontal alignment in all directions. Specifically, the intermediate suspension base and lower levelling base are connected via a triangular hinge structure and four hydraulic cylinders respectively. Two lateral hydraulic cylinders are symmetrically arranged about the seat's longitudinal center plane to ensure lateral levelling, while two longitudinal hydraulic cylinders are symmetrically positioned about the seat's transverse center plane to achieve longitudinal levelling.

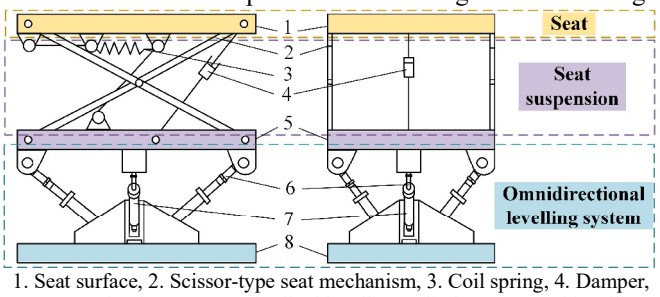

1. Seat surface, 2. Scissor-type seat mechanism, 3. Coil spring, 4. Damper, 5. Suspension base, 6. Longitudinal levelling cylinder, 7. Lateral levelling cylinder, 8. Levelling base.

Fig.1. Structure of the seat posture omnidirectional levelling system

To more clearly illustrate the relationship between seat tilt angle and seat geometric parameters, the complex structure depicted in Fig. 1 has been simplified. Figure 2 shows the simplified levelling system structure. Points O and C represent the fixed central points of the seat posture omnidirectional levelling system. Points D, E, F, and G represent the mounting points of the lateral and longitudinal hydraulic cylinders on the

levelling base. Points A, B, H, and I denote the mounting points of the lateral and longitudinal hydraulic cylinders on the suspension base. Points A' and B' correspond to points A and B after tilting θ_l, while points H' and I' correspond to points H and I after tilting θ_v. ϕ_0 denotes the initial angle between CA and CD, while ϕ_1 denotes the initial angle between CH and CF.

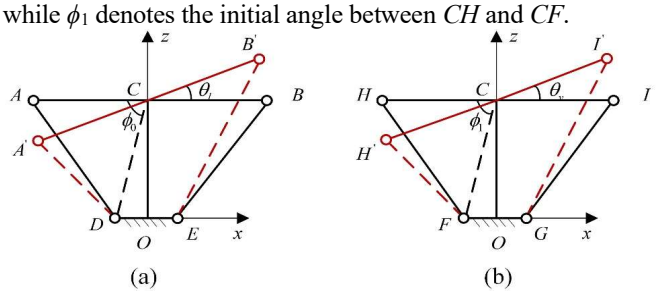

Fig.2. Structure of the levelling system: a) lateral, b) longitudinal

Taking the lateral direction as an example, prior to tilt (θ_l = 0°), in triangle ACD:

$$(AD)^2 = (CA)^2 + (CD)^2 - 2(CA)(CD)\cos\phi_0 \quad (1)$$

After tilting (by angle θ_l), the angle becomes (ϕ_0 - θ_l). Similarly:

$$(A'D)^2 = (CA')^2 + (CD)^2 - 2(CA')(CD)\cos(\phi_0 - \theta_l) \quad (2)$$

Subtracting formulas (1) and (2) and employing geometric formulas ultimately yields the expression for lateral tilt angle in terms of hydraulic cylinder displacement:

$$\theta_l = \arcsin\left(\frac{(AD + Y_0)^2 - (AD)^2}{2(CA)(CD)} - \frac{Y_0}{(CA)} \cdot \frac{\cos\phi_0}{\sin\phi_0}\right) \quad (3)$$

where Y_0 is the displacement of the lateral hydraulic cylinder, Y_0=($A'D$)-(AD), in mm.

Similarly, the expression for the longitudinal tilt angle and the hydraulic cylinder displacement can be derived:

$$\theta_v = \arcsin\left(\frac{(HF + Y_1)^2 - (HF)^2}{2(CH)(CF)} - \frac{Y_1}{(CH)} \cdot \frac{\cos\phi_1}{\sin\phi_1}\right) \quad (4)$$

where Y_1 denotes the displacement of the longitudinal hydraulic cylinder, Y_1=($H'F$)-(HF), in mm.

According to formulas (3) and (4), the displacement of the lateral and longitudinal hydraulic cylinders can be converted into the corresponding seat tilt angle.

The ideal seat tilt angles refer to the posture where the seat plane is perpendicular to the direction of gravity, meaning the normal vector of the seat plane aligns with the gravitational vector. At this point, both θ_l and θ_v are 0°. During actual operations in hilly terrain, as the tractor continuously traverses undulating landscapes, the vehicle's posture undergoes dynamic changes. Consequently, the ideal seat tilt angles (θ_l, θ_v) are not fixed values but rather time-varying dynamic target signals.

Equations (1–4) are derived from geometric relationships without trigonometric linearization and are applicable within the typical operating inclination ranges encountered in hilly terrain (lateral ±15°, longitudinal ±20°). These equations are formulated under the assumption that lateral and longitudinal tilts are considered independently. Under compound inclination conditions, coupled kinematic relationships should be analyzed, resulting in a more complex geometric model.

2.2. Hydraulic circuit design for seat posture omnidirectional levelling system

To ensure the hydraulic circuit of the seat posture omnidirectional levelling system achieves the anticipated load-bearing capacity and dynamic response performance, this section shall first elucidate its operating principle. Subsequently, based on this principle, the core parameters of the actuator's lateral and longitudinal levelling hydraulic cylinders (including cylinder bore and piston rod diameter) and the power source (working pressure and flow rate of the hydraulic pump) shall be designed. The direct objective of this series of design tasks is to provide precise parameter specifications for the system, thereby ensuring its capability to achieve omnidirectional, stable, and rapid levelling functionality.

The hydraulic operating principle of the seat posture omnidirectional levelling system is illustrated in Fig.3. The levelling system primarily comprises electromagnetic proportional directional control valves and hydraulic cylinders. The levelling system employs solenoid valves to regulate the inflow or outflow of hydraulic oil into the cylinder. When the control current is positive, the high-pressure source forces oil into the hydraulic cylinder; when the control current is negative, the oil flows in the opposite direction. TL and TR denote the left and right lateral levelling hydraulic cylinders responsible for seat lateral adjustment respectively; V-TL and V-TR denote the left and right three-position four-way solenoid proportional directional control valves for the lateral levelling cylinders respectively; DF and DB denote the front and rear longitudinal levelling cylinders respectively; V-DF and V-DB denote the three-position four-way electro-proportional directional valves for the front and rear longitudinal levelling cylinders respectively. For lateral levelling, the electromagnetic proportional directional valves V-TL and V-TR control the oil flow into and out of the hydraulic cylinders TL and TR. When oil enters the rodless chamber of TR and the rod chamber of TL, while oil exits the rod chamber of TR and the rodless chamber of TL, the right of the seat rises; conversely, the left rises. For longitudinal levelling, the hydraulic cylinders DF and DB are controlled via the proportional directional valves V-DF and V-DB. When oil enters the rodless chamber of DB and the rod chamber of DF, while oil exits the rod chamber of DB and the rodless chamber of DF, the back of the seat rises. Conversely, the front rises.

The omnidirectional seat levelling system designed in this paper employs independent lateral and longitudinal control. During lateral levelling, the controller calculates control signals based on lateral inclination error, driving electro-hydraulic proportional directional valves V-TL and V-TR

respectively to independently control the movement of the left hydraulic cylinder TL and right hydraulic cylinder TR, thereby achieving synchronous symmetrical adjustment of the left and right cylinders. At this stage, the front and rear hydraulic cylinders DF and DB operate in a follow-up state and are not actively controlled. During longitudinal levelling, the controller generates control signals based on longitudinal tilt error. These signals drive electro-hydraulic proportional directional valves V-DF and V-DB to synchronously and symmetrically control the front and rear hydraulic cylinders DF and DB respectively. Concurrently, the left and right hydraulic cylinders TL and TR remain in a trailing state and are not actively controlled.

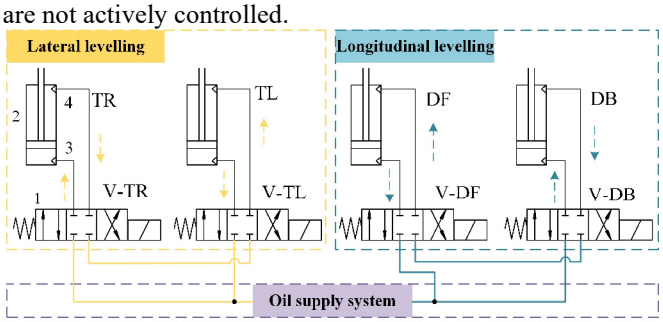

1. Electro-proportional directional valve, 2. Hydraulic cylinder, 3. Rodless chamber, 4. Rod chamber.

Fig.3. Hydraulic working principle of the seat posture omnidirectional levelling system

To ensure the load-bearing capacity and safety of the hydraulic cylinders, the maximum external load on the lateral levelling hydraulic cylinder shall not be less than 1500 N, and the maximum external load on the longitudinal levelling hydraulic cylinder shall not be less than 2000 N. For double-acting single-rod hydraulic cylinders, the cylinder remains under pressure throughout the levelling process. The active output force F of the hydraulic cylinder can be expressed as:

$$F = P_1 A_1 - P_2 A_2 \tag{5}$$

where:

$$A_1 = \frac{\pi}{4} D^2 \tag{6}$$

$$A_2 = \frac{\pi}{4}\left(D^2 - d^2\right) \tag{7}$$

where F denotes the driving force output by the hydraulic cylinder, in N; A_1 represents the effective piston area of the rodless chamber, in mm²; A_2 represents the effective piston area of the rod chamber, in mm²; P_1 denotes the pressure in the rodless chamber of the hydraulic cylinder, in MPa; P_2 denotes the pressure in the rod chamber of the hydraulic cylinder, in MPa; D denotes the piston diameter, mm; d denotes the piston rod diameter, in mm.

The initial working chamber pressure of the hydraulic cylinder is set at 2.5 MPa, while the return oil chamber pressure is 0 MPa. According to formula (5), the inner diameter of the hydraulic cylinder is:

$$D = \sqrt{\frac{4F}{\pi P_1}} \tag{8}$$

According to the Mechanical Design Handbook, the diameter of the hydraulic cylinder piston rod is:

$$d = 0.7D \tag{9}$$

From formulas (8) and (9), the diameter of the lateral levelling hydraulic cylinder is 27.6 mm with a piston rod diameter of 19.3 mm, while the longitudinal levelling cylinder has a diameter of 31.9 mm and a piston rod diameter of 22.3 mm. Ultimately, in accordance with national standard GB/T 2348-2018, the lateral levelling cylinder diameter is selected as 32 mm with a piston rod diameter of 20 mm; The longitudinal levelling hydraulic cylinder diameter is 40 mm, with a piston rod diameter of 25 mm.

Based on the hydraulic cylinder bore and piston rod diameter, the system working pressure P is determined as:

$$P_1 = \frac{4F}{\pi D^2} \approx 1.6\text{MPa} \tag{10}$$

The working flow rate Q of the hydraulic system is:

$$Q = \frac{\pi\left(D^2 - d^2\right)v}{4} \tag{11}$$

where v denotes the rapid extension velocity of the hydraulic cylinder, in mm/s. Formula (11) is employed for the preliminary design of hydraulic systems and the selection of pumps, with the objective of determining the rated flow rate required from the hydraulic pump to satisfy the system's demands under the most demanding operating conditions (namely, single-cylinder extension at maximum design velocity).

Taking v = 200 mm/s, the working flow rate of the hydraulic system is calculated to be 9.2 L·min^{-1}.

From the system working pressure, the hydraulic pump working pressure P_s can be calculated as:

$$P_s \geq P_1 + \sum \Delta P \tag{12}$$

where $\Sigma\Delta P$ represents the pressure loss in the piping between the hydraulic pump and the hydraulic cylinder, taken as 0.2 MPa.

From the system working flow rate Q, the hydraulic pump flow rate Q_s can be calculated as:

$$Q_s \geq \lambda K Q \tag{13}$$

where λ is the multi-cylinder drive coefficient, selected as 2.8; K is the leakage coefficient, taken as 1.2.

According to formulas (12) and (13), the hydraulic pump operating pressure is determined to exceed 1.8 MPa, with an operating flow rate exceeding 30.91 L·min^{-1}. Table 2 presents the principal technical parameters of the seat posture omnidirectional levelling system.

TABLE 2. Key technical parameters of the seat posture omnidirectional levelling system

Parameter	Lateral	Longitudinal
Seat surface/m	0.4	0.5
Levelling layer height/m	0.2	0.2
Hydraulic pump working pressure/pa	2.0×10^6	2.0×10^6
Hydraulic pump operating flow rate/L·min^{-1}	5.55	5.55
Hydraulic cylinder original length/m	0.25	0.28
Hydraulic cylinder diameter/mm	32	40
Hydraulic cylinder piston rod diameter /mm	20	25
Effective piston area of the rod chamber/mm^2	490	765
Effective piston area of the rodless chamber/mm^2	804	1256

3. MODEL ESTABLISHMENT OF THE SEAT POSTURE OMNIDIRECTIONAL LEVELLING SYSTEM

This paper employs control of the input current to the electromagnetic proportional directional valve to regulate the flow rate and pressure of oil entering the hydraulic cylinder. To achieve precise control of the seat posture omnidirectional levelling system, the oil supply system is configured as a constant-pressure source system. The constant-pressure source system effectively suppresses pressure fluctuations during multi-cylinder coordinated operation, thereby ensuring stable system performance. Consequently, this section does not model the individual components of the oil supply system, focusing solely on modelling the seat valve-controlled hydraulic cylinder system.

There are numerous types and classification methods for hydraulic control systems. Based on different combinations of hydraulic amplifiers and actuators, they can be categorized into four types: valve-controlled cylinders, valve-controlled motors, pump-controlled cylinders, and pump-controlled motors. Among these, valve-controlled cylinders offer rapid response, high precision, and the widest range of applications [30,31]. Consequently, this paper undertakes mathematical modelling and analysis of valve-controlled asymmetric hydraulic cylinder systems. Servo valves currently in practical use predominantly employ four-way solenoid valves for the main valve section. This is a structurally symmetric valve, where the structural parameters of the inlet and return sides are identical. However, asymmetric hydraulic cylinders possess a piston rod on only one side, resulting in unequal chamber volumes. relative to the system, this disrupts the overall symmetry, altering the mechanical motion parameters of the actuator in both directions. To achieve satisfactory bidirectional control performance, both the mathematical model and control strategy, originally established based on symmetry, must be correspondingly modified.

Currently, mathematical modelling typically involves establishing the fundamental equations for both the solenoid valve and the hydraulic cylinder separately, followed by simplification to complete the process [32]. The valve-controlled asymmetric hydraulic cylinder levelling system is illustrated in Fig.4.

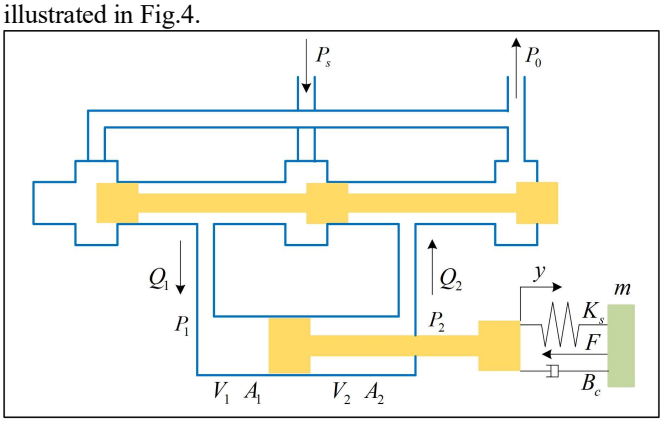

Fig.4. Valve-controlled asymmetric hydraulic cylinder levelling system

Continuity equation for the rodless and rod chamber flow of a hydraulic cylinder:

$$\begin{cases} Q_1 = C_i\left(P_1 - P_2\right) + C_e P_1 + \dfrac{V_1}{\beta_e}\dot{P}_1 + \dot{V}_1 \\ Q_2 = C_i\left(P_1 - P_2\right) - C_e P_2 - \dfrac{V_2}{\beta_e}\dot{P}_2 - \dot{V}_2 \end{cases} \tag{14}$$

where Q_1 denotes the flow rate in the rodless chamber of the hydraulic cylinder, in L·min^{-1}; Q_2 denotes the flow rate in the rod chamber of the hydraulic cylinder, in L·min^{-1}; C_i represents the internal leakage coefficient of the hydraulic cylinder; C_e represents the external leakage coefficient of the hydraulic cylinder; V_1 denotes the effective volume of the rodless chamber of the hydraulic cylinder, in m³; V_2 denotes the effective volume of the rod chamber of the hydraulic cylinder, in m³; β_e denotes the equivalent volumetric elastic modulus of the hydraulic oil, in MPa.

The force balance equation for a hydraulic cylinder is:

$$P_1 A_1 - P_2 A_2 = m\ddot{y} + B_c\dot{y} + K_s y + F \tag{15}$$

where m denotes the mass above the seat posture omnidirectional levelling system, in kg; y represents the displacement of the hydraulic cylinder, in m; B_c is the damping coefficient of the piston and load; K_s is the load spring stiffness, in N/m; F is the arbitrary time-varying external load force acting on the piston, in N.

It should be noted that in practical electro-hydraulic systems, friction may exhibit nonlinear characteristics at low velocities, such as Stribeck and stick–slip effects. In this study, friction is simplified and incorporated into the equivalent damping coefficient B_c, mainly representing viscous friction. Nonlinear friction may introduce small steady-state residual errors near zero velocity. However, the integral action of PID compensates steady-state bias, and the adaptive parameter

tuning mechanism of the proposed QBP-PID enhances robustness against moderate unmodelled nonlinearities.

Introducing auxiliary variables:

$$P_L = P_1 - \frac{A_2}{A_1} P_2 \tag{16}$$

$$Q_L = \frac{Q_1 + \frac{A_2}{A_1} Q_2}{1 + \frac{A_2}{A_1}} \tag{17}$$

where P_L is the load pressure; Q_L denotes the load flow rate.

The flow equation of the valve is the key link between the hydraulic circuit and the mechanical motion of the spool. The generalized flow formula for a spool valve can be expressed as [33]:

$$Q = C_t \omega x \sqrt{\frac{2}{\rho} \Delta P} \tag{18}$$

where C_t represents the flow coefficient; ω is the gradient in the spool valve area; ρ denotes the oil density, in kg/m³; x represents the displacement of the solenoid valve spool, in m.

The parameter values in the above equations are shown in Table 3.

TABLE 3. The parameter values in the above equations

Parameter	Symbol	Value
Flow coefficient	C_t	0.61
Area gradient of the spool area	ω	0.235
Hydraulic oil density kg/m³	ρ	850
Equivalent volumetric modulus of elasticity for hydraulic oil/MPa	β_e	6.8×10^2
External leakage coefficient of hydraulic cylinder	C_e	0
Internal leakage coefficient of hydraulic cylinder	C_i	3×10^{-6}
Mass above the seat posture omnidirectional levelling system/kg	m	150

In valve-controlled hydraulic cylinder systems, variations in the internal leakage coefficient C_i and the equivalent volumetric elastic modulus β_e of the hydraulic fluid significantly impact hydraulic system performance. C_i reflects leakage at the piston seal (piston seal area), primarily reducing the system's static stiffness. This is equivalent to increasing the system's damping, potentially resulting in reduced overshoot during step responses but slower response speeds. β_e reflects the compressibility of the hydraulic fluid. The ingress of air into the fluid or an increase in temperature will cause β_e to decrease, slowing dynamic responses and potentially inducing resonance. The external leakage coefficient C_e is set to 0 in this paper is not a theoretical absolute assumption. Rather, during normal system operation, the influence of C_e on system dynamics is a higher-order negligible quantity compared to C_i and β_e. Consequently, it is reasonably omitted in the controller design model.

By linearizing equation (18) at the zero-position operating point, a linear expression is obtained between the load flow Q_L and the valve spool displacement x, load pressure P_L:

$$Q_L = K_q x - K_c P_L \tag{19}$$

where:

$$K_q = \left.\frac{\partial Q_L}{\partial x_v}\right|_0, K_c = -\left.\frac{\partial Q_L}{\partial P_L}\right|_0$$

where K_q is the flow velocity gain coefficient; K_c denotes the pressure gain coefficient.

Performing a Laplace transform on equation (15), then substituting equation (16) and assuming the external load force $F(s) = 0$, yields:

$$\left(ms^2 + B_c s\right) Y(s) = A_1 P_L(s) \tag{20}$$

Furthermore, applying the Laplace transform to equation (14) and substituting into equation (17), then simplifying using the relationship in equation (16), yields another expression for the load flow Q_L:

$$Q_L(s) = A_1 s Y(s) + C_d P_L(s) + \frac{V_t}{4\beta_e} s P_L(s) \tag{21}$$

where:

$$C_d = C_i\left(1 + \left(\frac{A_2}{A_1}\right)^2\right), V_t = V_1 + \left(\frac{A_2}{A_1}\right) V_2$$

where C_d denotes the total leakage coefficient; V_t represents the equivalent volume.

Performing the Laplace transform on equation (19) and combining it with equation (21) to eliminate $Q_L(s)$ yields:

$$K_q X_v(s) - K_c P_L(s) = A_1 s Y(s) + C_d P_L(s) + \frac{V_t}{4\beta_e} s P_L(s) \tag{22}$$

By combining Equations (20) and (22) to eliminate the intermediate variable $P_L(s)$ and rearranging the resulting equation, the transfer function of the valve-controlled hydraulic cylinder, which relates the valve spool displacement $X(s)$ (input) to the cylinder displacement $Y(s)$ (output), is derived as follows:

$$G_1(s) = \frac{Y(s)}{X(s)} = \frac{\frac{K_q}{A_1}}{s\left(\frac{s^2}{\omega_h^2} + \frac{2\xi_h}{\omega_h} s + 1\right)} \tag{23}$$

where:

$$\omega_h = \sqrt{\frac{4\beta_e A_1^2}{V_t m}}, \xi_h = \frac{K_c + C_d}{A_1}\sqrt{\frac{\beta_e m}{V_t}} + \frac{B_c}{4A_1}\sqrt{\frac{V_t}{\beta_e m}}$$

where ω_h denotes the natural frequency of the hydraulic cylinder; ξ_h represents the damping ratio of the hydraulic cylinder.

The transfer function of the solenoid valve is [34]:

$$G_2(s) = \frac{X(s)}{I(s)} = \frac{K_v}{\frac{s^2}{\omega_v} + \frac{2\xi_v}{\omega_v}s + 1} \tag{24}$$

where K_v denotes the gain coefficient of the solenoid valve's electromagnet, in m/A; ω_v represents the natural frequency of the electromagnet, in rad/s; and ξ_v signifies the damping ratio of the electromagnet.

The transfer function obtained after connecting the hydraulic cylinder and the solenoid valve in series, with the solenoid valve current as the input and the hydraulic cylinder displacement as the output, is:

$$\begin{aligned} G(s) &= G_1(s)\cdot G_2(s) = \frac{Y(s)}{I(s)} \\ &= \frac{\frac{K_q K_v}{A_1}}{s\left(\frac{s^2}{\omega_h^2} + \frac{2\xi_h}{\omega_h}s + 1\right)\left(\frac{s^2}{\omega_v^2} + \frac{2\xi_v}{\omega_v}s + 1\right)} \end{aligned} \tag{25}$$

Stability analysis of the designed levelling system was conducted using MATLAB. The Bode diagram is shown in Fig. 5. It can be observed that the amplitude margin and phase margin are 5.19 dB and 25.1°, respectively. According to classical control theory, a control system is generally considered stable when both the amplitude margin and phase margin are positive. Therefore, the designed single hydraulic cylinder system possesses good stability and strong interference resistance.

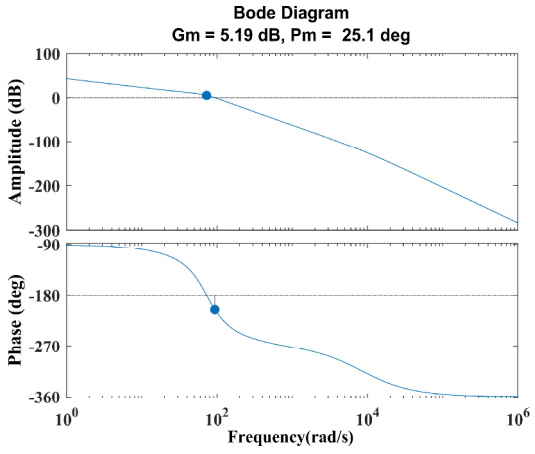

Fig.5. Bode diagram

The above stability analysis is conducted for a single hydraulic cylinder subsystem. In the practical omnidirectional levelling system, mechanical coupling between lateral and longitudinal cylinders may occur. However, the system adopts independent control channels with symmetric cylinder configurations. During single-direction levelling, the orthogonal cylinders operate in a follow-up state, reducing dynamic cross-interaction.

From a control perspective, coupling effects can be regarded as bounded disturbances acting on each subsystem. Since each hydraulic loop exhibits sufficient gain and phase margins, the overall closed-loop system maintains practical stability under moderate coupling conditions.

Formula (25) represents a high-order complex model, rendering its direct application in controller design rather cumbersome. To simplify analysis and highlight the dominant dynamics, whilst facilitating subsequent discretization and digital controller implementation, the model undergoes appropriate order reduction. This ultimately yields the state-space equations of the continuous-time levelling system:

$$\begin{cases} x(t+1) = A_d x(t) + B_d I(t) \\ y(t) = C_d x(t) \end{cases} \tag{26}$$

where:

$$A_d = \begin{bmatrix} 0 & 1 & 0 \\ 0 & 0 & 1 \\ 0 & -\frac{1}{T_v T_h} & -\frac{T_v + T_h}{T_v T_h} \end{bmatrix}, B_d = \begin{bmatrix} 0 \\ 0 \\ \frac{K}{T_v T} \end{bmatrix}, C_d = \begin{bmatrix} 1 & 0 & 0 \end{bmatrix}$$

where:

$$K = \frac{K_v K_q}{A_1}, T_v = \frac{1}{\omega_v}, T_h = \sqrt{\frac{V_t m}{4\beta_e A_1^2}}$$

Discretization of equation (26) using Euler's method yields the state-space equation in discrete form:

$$\begin{cases} x(k+1) = A_{d,k} x(k) + B_{d,k} I(k) \\ y(k) = C_{d,k} x(k) \end{cases} \tag{27}$$

where:

$$A_{d,k} = \begin{bmatrix} 1 & T_s & 0 \\ 0 & 1 & T_s \\ 0 & -\frac{T_s}{T_v T_h} & 1 - \frac{T_s(T_v + T_h)}{T_v T_h} \end{bmatrix}, B_{d,k} = \begin{bmatrix} 0 \\ 0 \\ \frac{T_s K}{T_v T_h} \end{bmatrix},$$

$$C_{d,k} = C_d = \begin{bmatrix} 1 & 0 & 0 \end{bmatrix}$$

where T_s is the sampling time.

4. USING THE TEMPLATE DESIGN OF QBP-PID OMNIDIRECTIONAL RAPID LEVELLING CONTROL STRATEGY

The difficulty with classical PID control lies in the parameter design of proportional, integral, and derivative gains. Moreover, once parameters are determined, they cannot be adjusted online, rendering the control performance incapable of adapting to environmental changes [35]. For the seat levelling system studied in this paper, such variations primarily include: 1) Differences in driver weight; 2) Changes in the dynamic target signals (ideal tilt angle). This paper employs the self-learning capability of BP neural network to perform real-time updates of PID control parameters, thereby addressing the challenge of PID parameter tuning [36]. However, the introduction of neural network in BP-PID results in prolonged algorithm training times, and the difficulty in determining connection weights between neurons across layers constrains the algorithm's performance. This paper fuses BP neural network with the Q-learning algorithm to design a QBP-PID strategy for rapid omnidirectional levelling control of seat posture. Q-learning requires no specific model consideration, possesses strong autonomous exploration capabilities, and can effectively perform parameter search and tuning [27]. Meanwhile, the BP neural network, with its self-learning ability, can achieve non-linear mapping of models. Introducing the BP neural network enables online real-time optimization of PID control parameters, while the Q-learning algorithm updates the connection weights of the BP neural network in real time. The QBP-PID control algorithm, formed by the combination of these three algorithms, can resolve the issue of poor parameter adaptation in traditional PID control.

The control rate expression for the classic PID controller is:

$$I(t) = K_P e(t) + K_I \int e(t)dt + K_D \frac{de(t)}{dt} \quad (28)$$

where K_P is the proportional gain; K_I denotes the integral gain; K_D represents the derivative gain.

After simultaneously differentiating both sides of the continuous-time PID equation and subsequently discretizing it, the control rate expression for the discrete-time BP-PID controller is obtained as follows:

$$\begin{aligned} I(k) = {} & I(k-1) + K_P(e(k) - e(k-1)) \\ & + \frac{K_I T_s}{2}(e(k) + e(k-1)) + K_D(e(k) \\ & -2e(k-1) + e(k-2)) \end{aligned} \quad (29)$$

Express the state-space equation of the levelling system as:

$$y(k+1) = \lambda(x(k+1), I(k)) \quad (30)$$

where $\lambda(\cdot)$ is the levelling system control function.

The BP neural network employs a three-layer architecture with 3-6-3 nodes. The input layer comprises three nodes, the single hidden layer contains six nodes, and the output layer consists of three nodes. The three input layer nodes are denoted as x_i (i = 1, 2, 3). Inputs $e(k)$, $e(k)$ - $e(k\text{-}1)$, and $e(k)$ - $2e(k\text{-}1)$ + $e(k\text{-}2)$ undergo normalization processing before being fed as inputs x_i. The number of output layer nodes relates to the actual controlled object. The neural network's hidden layer outputs are $O_j(k)$, corresponding to the three control parameters of PID control. The output layer outputs are $O_k(k)$, calculated as follows:

$$\begin{cases} O_j(k) = f_1\left[\sum_{j=1}^{6} \omega_{ij} x_i - \theta_j\right] \\ O_k(k) = f_2\left[\sum_{j=1}^{6} \omega_{jk} O_j(k) - \theta_k\right] \end{cases} \quad (31)$$

where ω_{ij} is the connection weight between the input layer and the hidden layer neuron nodes; ω_{jk} denotes the connection weight between the output layer and the hidden layer neuron nodes; θ_j represents the bias of the jth neuron in the hidden layer; θ_k is the bias of the kth neuron in the output layer; $f_1(\cdot)$ and $f_2(\cdot)$ are the activation functions.

The Sigmoid function is selected as the activation function, and its expression is:

$$\begin{cases} f_1 = \dfrac{2}{1+e^x} - 1 \\ f_2 = \dfrac{1}{1+e^x} \end{cases} \quad (32)$$

The control gain for the QBP-PID is:

$$\begin{cases} K_P = O_1 \\ K_I = O_2 \\ K_D = O_3 \end{cases} \quad (33)$$

For the seat posture omnidirectional levelling system, the performance indicator function J is defined as:

$$J = \sum_{k=1}^{N} J_k = \sum_{k=1}^{N} \left[e^T(k+1) Q_k e(k+1) + I^T(k) R_k I(k) \right] \quad (34)$$

where N is the total time step; Q_k and R_k are the connection weight matrix.

The connection weights $\omega_{ij}(k)$ and $\omega_{jk}(k)$ of the BP neural network are updated using the gradient descent method [37]:

$$\begin{cases} \omega_{ij}(k+1) = \omega_{ij}(k) - \eta[1-\psi(k)]\dfrac{\partial J_k}{\partial \omega_{ij}(k)} + \psi(k)\dfrac{\partial J_k}{\partial \omega_{ij}(k)} \\ \omega_{jk}(k+1) = \omega_{jk}(k) - \eta[1-\psi(k)]\dfrac{\partial J_k}{\partial \omega_{jk}(k)} + \psi(k)\dfrac{\partial J_k}{\partial \omega_{jk}(k)} \end{cases} \quad (35)$$

where η is the learning rate, $\eta > 0$; $\psi(k)$ represents the momentum factor, $0 < \psi(k) < 1$.

Since the error state x_i in PID control fully reflects the system's dynamic requirements, aligning perfectly with the input layer of BP neural network while offering reduced dimensionality, the momentum factor $\psi(k)$ effectively suppresses frequent oscillations during the learning process, enhancing learning efficiency. As a scalar within the range [0,1], it minimizes the action space. Therefore, in the Q-learning algorithm design, the momentum factor $\psi(k)$ is treated as the action set, while the QBP-PID inputs $x_i(i=1,2,3)$ constitute the state set.

For the Q-learning algorithm, the reward function determines the optimal sequence of actions. By setting an input-related reward function, the action strategy at each time step is established. An ideal control outcome is achieved when the seat tilt angle error $e(k) = 0°$. Therefore, reducing the error $e(k)$ is treated as a reward, prompting learning adjustments in that direction. Conversely, increasing the error is treated as a penalty, prompting learning adjustments in the opposite direction. The reward function is defined as:

$$R_i = -\left[e(k) - 0\right]^2 \tag{36}$$

Based on the design of Q-learning's state, action, and reward, the current levelling system selects the action with the maximum Q value. It calculates the reward obtained during the update process and dynamically adjusts connection weights by updating the Q table. The iterative Q value equation for Q-learning can be expressed as:

$$Q^{k+1}(s_k,a_k) = Q^k(s_k,a_k) + \alpha\left[R(s_{k+1},a_k) + \gamma \max Q^k(s_{k+1},a_k) - Q^k(s_k,a_k)\right] \tag{37}$$

where $Q^k(s_k,a_k)$ is the Q value of action a_k in state s_k; α represents the learning rate; γ is the discount factor; and $R(s_{k+1},a_k)$ signifies the reward value under action a_k.

Following the completion of the Q-learning design, the online real-time parameter collection and dynamic optimization of the QBP-PID are implemented according to the corresponding iterative steps. The specific process is illustrated in Fig.6.

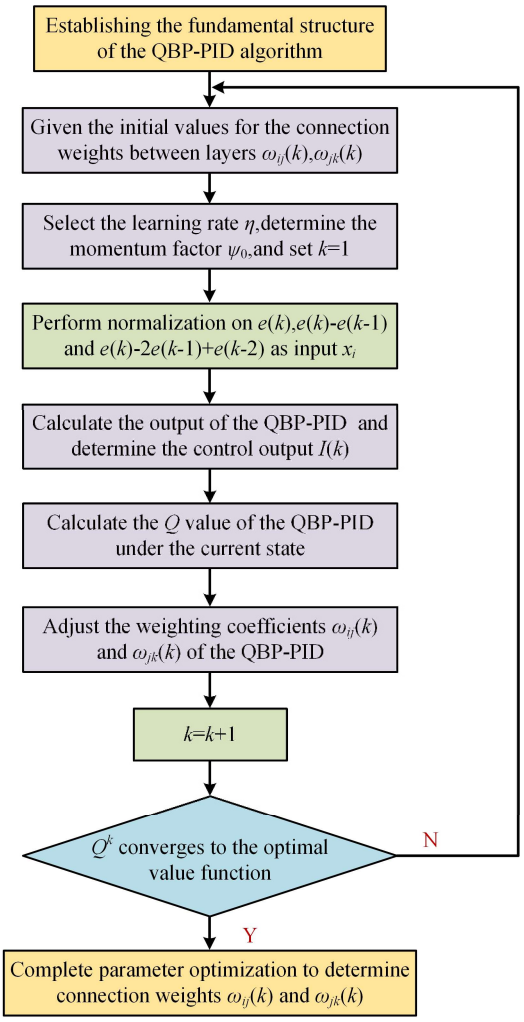

Fig.6. Dynamic optimization process for QBP-PID parameters

During the online operation of the QBP-PID system, both the BP neural network and Q-learning utilize error state x_i as inputs, with their synergistic interaction facilitated through the momentum term factor $\psi(k)$. The BP neural network performs forward calculations at each control cycle, outputting PID parameters K_P, K_I, and K_D, thereby calculating the solenoid valve control current $I(k)$ applied to the levelling system. Concurrently, the system's control performance is reflected in the performance indicator function J_k. J_k is converted into the reward R_i for Q-learning, which adjusts $\psi(k)$ based on this reward. Consequently, the connection weights $\omega_{ij}(k)$ and $\omega_{jk}(k)$ of the BP neural network are updated.

The principle of the QBP-PID omnidirectional rapid levelling control strategy is illustrated in Fig.7. $\theta_d(k)$ is the ideal seat tilt angle, $\theta(k)$ represents the actual seat tilt angle signal, $e(k)$ indicates the seat tilt angle error, $I(k)$ signifies the solenoid valve control current signal for the levelling system, and $Y(k)$ denotes the hydraulic cylinder displacement. The QBP-PID algorithm performs real-time online correction of the BP neural network connection weights $\omega_{ij}(k)$ and $\omega_{jk}(k)$ based on the $e(k)$. It outputs optimal PID control parameters K_P, K_I, and K_D, ultimately controlling the extension and retraction of the levelling system's hydraulic cylinder to achieve seat posture levelling control.

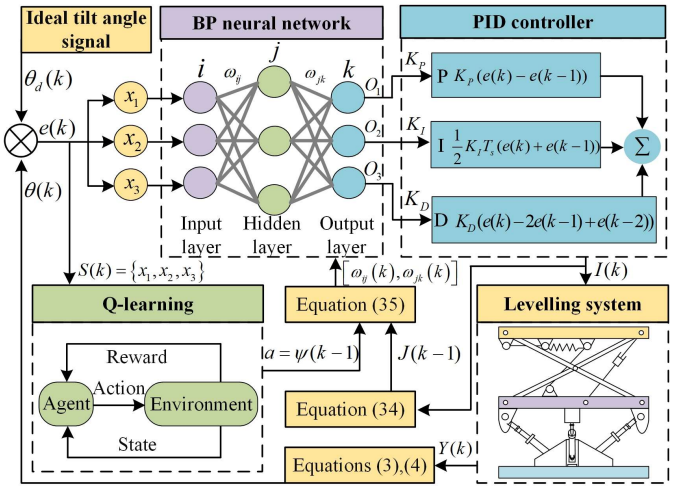

Fig.7. Principle of the QBP-PID omnidirectional rapid levelling control strategy

The specific control process for the QBP-PID omnidirectional rapid levelling control strategy is as follows:

(1) At time k, the error $e(k)$ between the actual seat tilt angle $\theta(k)$ and the desired seat tilt angle $\theta_d(k)$ is normalized and used as input x_i (i = 1, 2, 3).

(2) The connection weights $\omega_{ij}(k)$ and $\omega_{jk}(k)$ at time k are determined by the momentum factor $\psi(k\text{-}1)$ and the performance indicator function $J(k\text{-}1)$ from time (k-1), then input to the BP neural network.

(3) The outputs O_1, O_2, and O_3 from the output layer serve as the PID controller parameters K_P, K_I, and K_D respectively to calculate the control current signal $I(k)$ for the levelling system.

(4) The control current signal $I(k)$ governs the extension and retraction of the hydraulic cylinder, which outputs displacement $Y(k)$. Simultaneously, $I(k)$ update the performance function J through equation (31), thereby updating the connection weights for the subsequent control cycle. This concludes the control cycle at time k.

(5) The hydraulic cylinder displacement is reconverted into the actual seat tilt angle signal through equations (3) and (4), initiating the next control cycle for the levelling system.

Under time-varying disturbances, the QBP-PID adaptation mechanism operates within a closed-loop stable framework. The neural network weights are updated using gradient descent with a bounded learning rate and momentum factor $\psi(k) \in (0,1)$, ensuring bounded weight increments at each step. In addition, Q-learning selects the momentum factor from a finite action set, and under the standard update rule ($0 < \alpha < 1$ and $0 < \gamma < 1$), Q-values remain bounded.

It should be noted that bounded parameter updates do not imply strict convergence of the overall adaptive process. Instead, the proposed method ensures that parameter evolution remains bounded during online learning. In practical control scenarios, the adaptation process is driven by the error signal and exhibits stable adaptive behavior. Consequently, under moderate nonstationary disturbances and varying operating conditions, the controller maintains practical stability and robustness without parameter divergence during online operation.

5. SIMULATION RESULTS VERIFICATION AND ANALYSIS

Based on the MATLAB simulation platform, a model of the seat posture omnidirectional levelling system is established. Using the seat tilt angle signal as the controller input and the solenoid valve current signal as the controller output, a simulation platform for the omnidirectional levelling control system is constructed. Initial seat tilt angle signals of 15° laterally and 20° longitudinally are set, with the desired seat lateral/longitudinal tilt angles set to 0°. This yield seat tilt angle error e(k) in two directions, which are input to the QBP-PID controller. After controller operation, control signal for the hydraulic cylinder of levelling system are output, thereby adjusting the seat tilt angle. To validate the levelling performance of the proposed QBP-PID omnidirectional rapid levelling control strategy, BP-PID and PID control strategies are employed as comparative strategies. Control parameters are obtained through trial-and-error methods, as presented in Table 4.

TABLE 4. Control parameter configuration

Parameter	PID		BP-PID/QBP-PID	
	Lateral	Longitudinal	Lateral	Longitudinal
K_P	1.4	0.8	1.7	1.3
K_I	0.6	0.3	0.6	0.6
K_D	0.4	0.5	0.1	0

In this system design, the prioritizations of control performance are as follows: levelling time > overshoot > smoothness. That is, under the premise of ensuring stability, priority is given to reducing levelling time to minimize driver fatigue caused by sustained tilting, while simultaneously limiting overshoot to prevent secondary discomfort, and ensuring smooth motion to enhance overall comfort.

5.1. Lateral levelling

The initial lateral tilt angle was set to 15°, with a simulation duration of 10 seconds. The lateral simulation results are shown in Fig. 8 to Fig. 13.

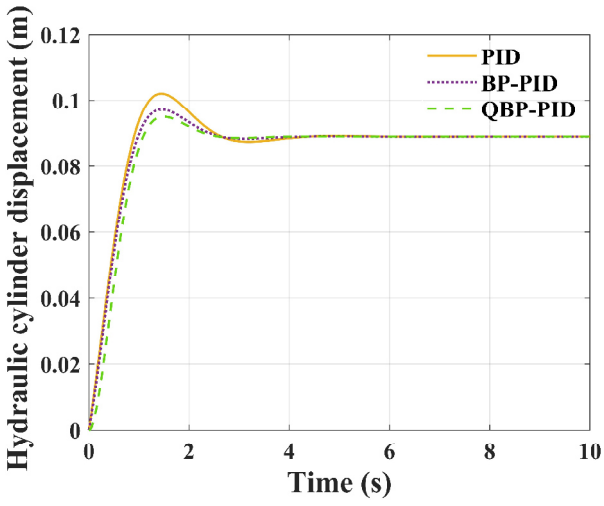

Fig.8. Lateral hydraulic cylinder displacement

Figure 8 depicts the displacement variation curve of the hydraulic cylinder during lateral levelling. As shown in Fig. 8, under PID control, the maximum displacement of the hydraulic cylinder reaches 0.102 m with an overshoot of 0.014 m, accompanied by oscillation; Under BP-PID control, the maximum displacement of the hydraulic cylinder is 0.097 m with an overshoot of 0.009 m; whereas under QBP-PID control, the maximum displacement is 0.094 m with an overshoot of 0.006 m; Both QBP-PID and BP-PID eliminated oscillations, but the QBP-PID exhibits a smaller displacement overshoot. Compared to BP-PID and PID control, displacement overshoot is reduced by 57.14% and 33.33%, respectively. This is because the QBP-PID control employs reinforcement learning to optimize BP neural network weights online, effectively minimizing displacement overshoot.

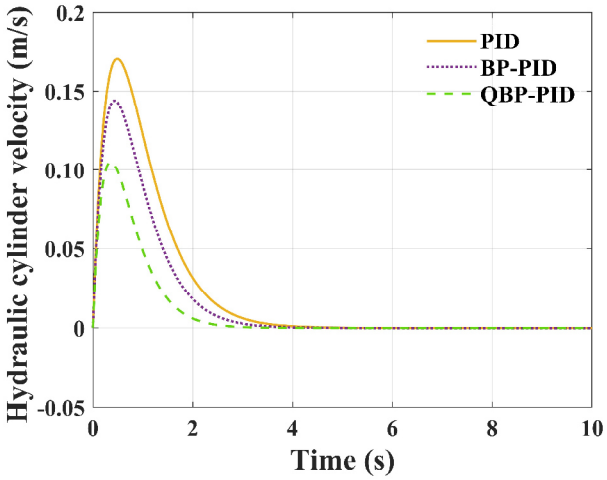

Fig.9. Lateral hydraulic cylinder velocity

Figure 9 is the hydraulic cylinder velocity variation curve during lateral levelling. As shown in Fig. 9, the hydraulic cylinder exhibits a high initial velocity. Under PID control, the maximum velocity reaches 0.17 m/s; under BP-PID control, the maximum velocity reaches 0.143 m/s; and under QBP-PID control, the maximum velocity is 0.105 m/s. Compared to BP-PID and PID control, the maximum velocity is reduced by 15.9% and 38.2%, respectively. Excessively rapid levelling velocity compromise driver comfort. By optimizing the BP neural network weights, the QBP-PID control devises an optimal velocity curve, thereby enhancing driver comfort.

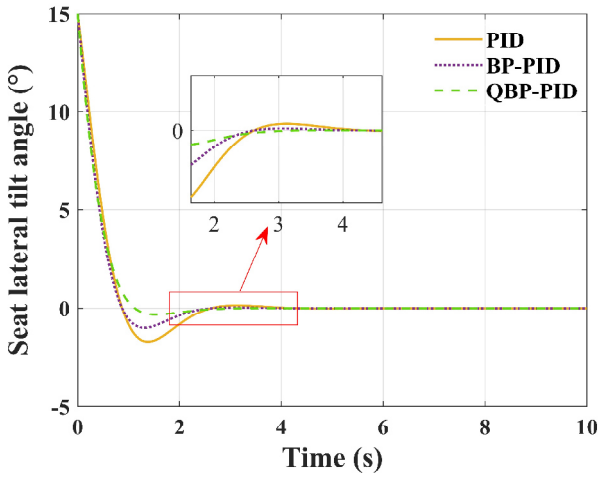

Fig.10. Seat lateral tilt angle

The variation in seat lateral tilt angle directly reflects lateral levelling performance. Figure 10 illustrates the seat lateral tilt angle curve during lateral levelling. It can be observed that under PID control, the lateral levelling time is 4.12 s, with an overshoot of 1.71° and oscillation occurring. Under BP-PID control, the lateral levelling time was 3.64 s with an overshoot of 1.01°. Under QBP-PID control, the lateral levelling time decreased to 2.98 s and the overshoot reduces to 0.32°. compared to BP-PID and PID, representing reductions of 18.13% and 27.66%, respectively. As demonstrated in Fig.8 and Fig. 9, the QBP-PID control effectively suppresses displacement overshoot, optimizes velocity planning, and achieves 'rapid and smooth' lateral levelling of the seat.

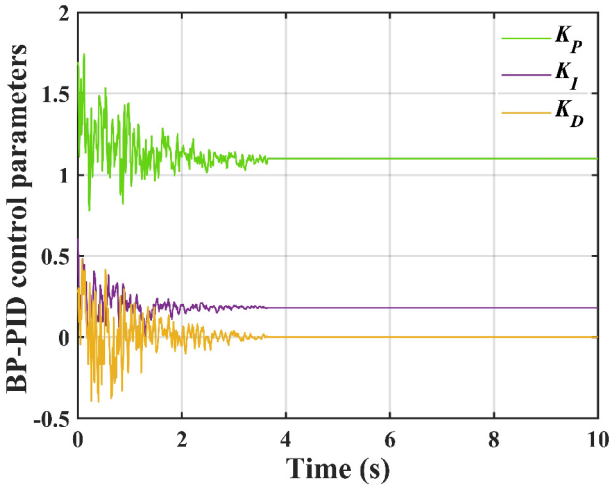

Fig.11. BP-PID control Parameters

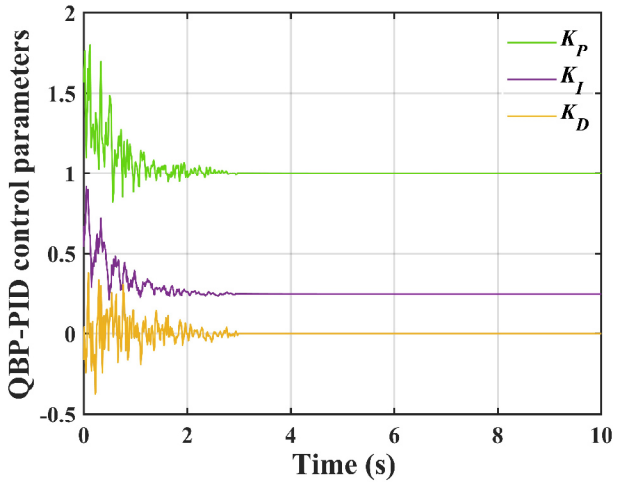

Fig.12. QBP-PID control Parameters

Figure 11 and Figure 12 show the control parameters variation curve during lateral levelling. As evident from Fig. 11, at the start of levelling, the initial values of the QBP-PID and BP-PID control parameters are the same. The BP-PID completed levelling at 3.64 s, with control parameters stabilizing at K_P = 1.1, K_I = 0.18, and K_D = 0. The QBP-PID concluded levelling at 2.98 s, maintaining control parameters at K_P = 1, K_I = 0.25, and K_D = 0. Comparing Fig. 11 and Fig. 12 reveals that, relative to BP-PID, the QBP-PID control parameters exhibit smoother and more stable variation throughout the lateral levelling process. This stems from the fact that while BP-PID updates control parameters by incorporating BP neural network, QBP-PID employs reinforcement learning to optimize the BP neural network weights online. This enables the control parameters to adapt more effectively to the lateral levelling conditions.

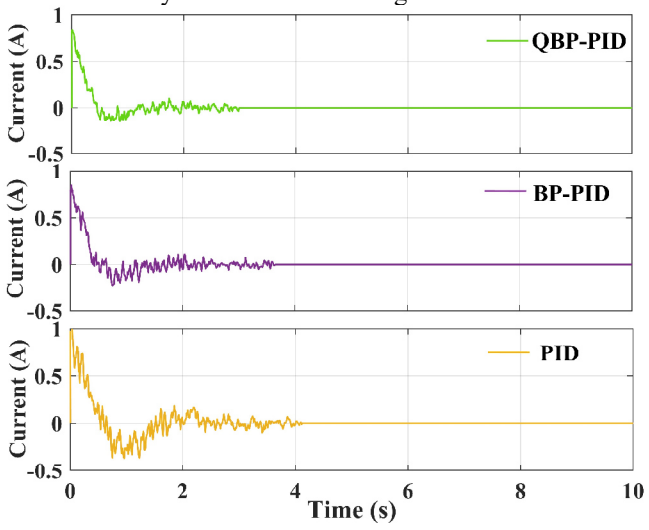

Fig.13. Solenoid valve control current

Figure 13 shows the variation curve of the solenoid valve control current during lateral levelling. As evident from Fig. 12, the solenoid valve control current decreases as the seat tilt angle diminishes. Both QBP-PID and BP-PID exhibit the same peak currents of 0.82 A. Compared to PID, the peak current is reduced by 18%. However, the QBP-PID control strategy delivers the smoothest current response. This demonstrates that the Q-learning algorithm effectively optimizes the BP neural network weights, resulting in more precise and stable control current outputs.

5.2. Longitudinal levelling

The initial longitudinal tilt angle is set to 20°, and the longitudinal simulation results are shown in Fig. 14 to Fig. 19.

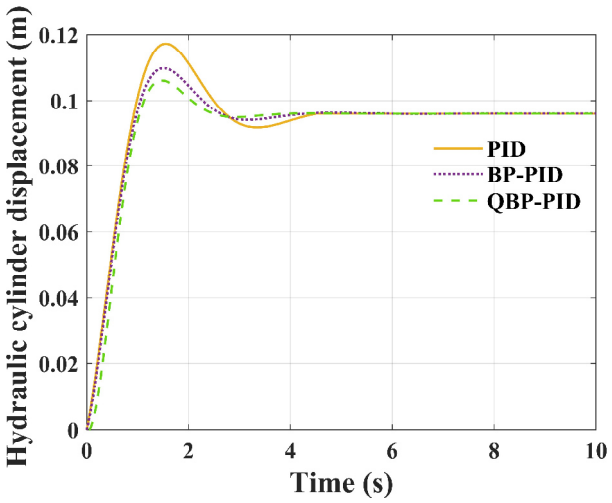

Fig.14. Longitudinal hydraulic cylinder displacement

Figure 14 is the displacement variation curve of the hydraulic cylinder during longitudinal levelling. It can be observed that under PID control, the maximum displacement of the hydraulic cylinder reaches 0.117 m, with an overshoot of 0.021 m and oscillation occurring; Under BP-PID control, the maximum displacement of the hydraulic cylinder is 0.109 m with an overshoot of 0.013 m, also exhibiting oscillations; whereas under the QBP-PID control, the maximum displacement is 0.105 m with an overshoot of 0.009 m. Compared to BP-PID and PID control, the QBP-PID eliminates oscillations, with overshoot being reduced by 30.76% and 57.14%, respectively. This is due to the QBP-PID control effectively reducing longitudinal hydraulic cylinder displacement overshoot by optimizing the BP neural network weights.

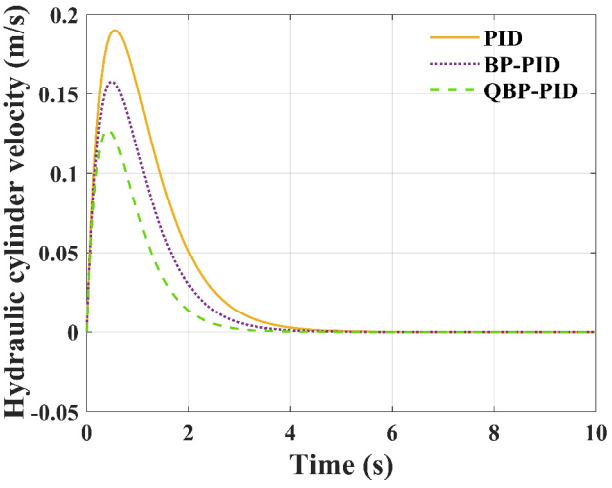

Fig.15. Longitudinal hydraulic cylinder velocity

Figure 15 shows the hydraulic cylinder velocity variation curve during longitudinal levelling. As evident from Fig. 14, the

hydraulic cylinder velocity is relatively high at the start of levelling. Under PID control, the maximum velocity reaches 0.189 m/s; under BP-PID control, it peaks at 0.157 m/s; and under QBP-PID control, the maximum velocity is 0.127 m/s. Compared to BP-PID and PID control, the maximum velocity is reduced by 19.1% and 32.8%, respectively. Excessively rapid levelling velocity can also cause discomfort to the driver. The QBP-PID control enhances driver comfort by optimizing the BP neural network weights and dynamically adjusting the optimal hydraulic cylinder velocity.

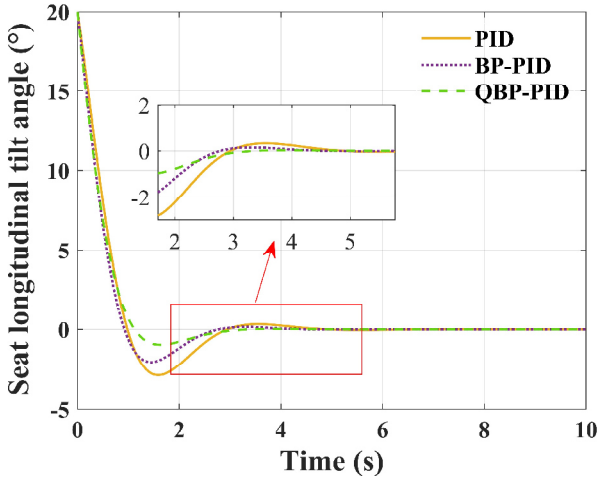

Fig.16. Seat longitudinal tilt angle

Figure 16 is the variation curve of the seat's longitudinal tilt angle during longitudinal levelling. It can be observed that under PID control, the seat's longitudinal levelling time is 4.59 s, with an overshoot of 2.87° and oscillation occurring. Under BP-PID control, the seat's longitudinal levelling time is 4.14 s, with an overshoot of 2.04°, and oscillation similarly occurs. whereas under QBP-PID control, the longitudinal levelling time is reduced to 3.41 s with overshoot diminished to 0.95°, eliminating oscillations. Compared to BP-PID and PID, the longitudinal levelling time is reduced by 17.63% and 31.6%, respectively. Combining Fig. 14 and Fig. 15 reveals that the QBP-PID control effectively suppresses displacement overshoot, optimizes velocity planning, and achieves 'rapid and smooth' longitudinal levelling of the seat.

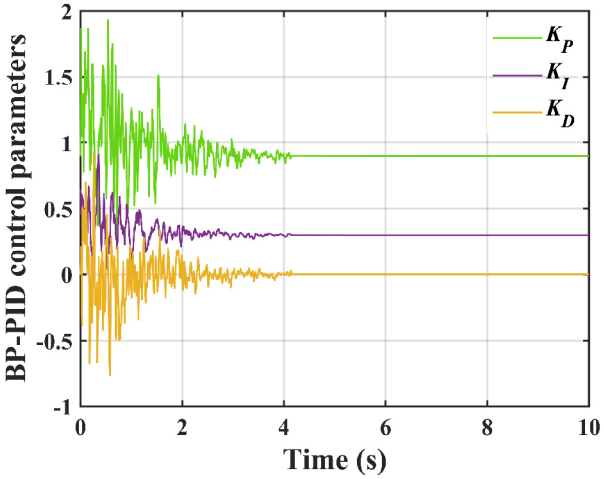

Fig.17. BP-PID control parameters

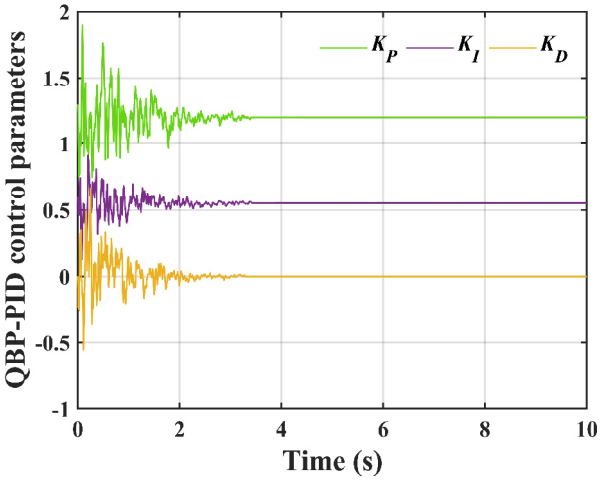

Fig.18. QBP-PID control parameters

Figure 17 and Figure 18 depict the control parameters variation curves during longitudinal levelling. It can be observed that at the beginning of levelling, the initial values of the QBP-PID and BP-PID control parameters are the same, with BP-PID completing levelling at 4.14 s, maintaining control parameters at $K_P = 0.9$, $K_I = 0.3$, and $K_D = 0$; QBP-PID completes levelling at 3.41 s, with control parameters stabilizing at $K_P = 1.2$, $K_I = 0.55$, $K_D = 0$. Comparing Fig. 17 and Fig. 18 reveals that the QBP-PID exhibits smoother and more stable control parameters throughout the levelling process compared to BP-PID.

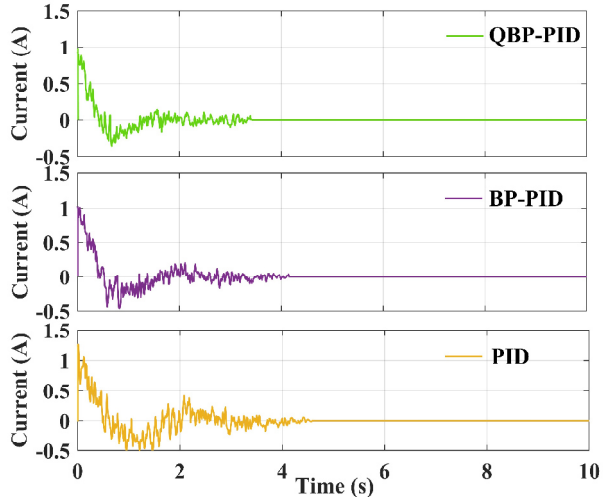

Fig.19. Solenoid valve control current

Figure 19 depicts the solenoid valve control current variation curve during longitudinal levelling. When considered alongside Fig. 16, it is evident that the solenoid valve control current exhibits the same variation trends to the seat's longitudinal tilt angle. Both the QBP-PID and BP-PID achieve identical peak currents of 1 A. Compared to the PID, the peak current is reduced by 23%. However, the QBP-PID control strategy delivers the smoothest current response relative to the BP-PID and PID.

In summary, during both lateral and longitudinal seat levelling, the QBP-PID omnidirectional rapid levelling control strategy demonstrates significant superiority over the BP-PID

and PID control strategies in both response speed and control accuracy. This effectively enhances driver comfort, providing an advanced and effective solution for improving the omnidirectional levelling performance of tractor seat in hilly and mountainous terrain.

6. CONCLUSIONS

To address the diminished comfort experienced by tractor driver in hilly and mountainous terrain due to vehicle tilt, a novel seat posture omnidirectional levelling system is designed and a QBP-PID omnidirectional rapid levelling control strategy for seat posture is proposed in this paper. Using the BP-PID and PID as comparison strategies, simulation experiments are conducted on the QBP-PID omnidirectional rapid levelling control strategy based on the MATLAB simulation platform, validating its effectiveness. The main conclusions of this study are as follows:

(1) At a lateral tilt angle of 15°, the lateral levelling time under the PID control is 4.12 s, under the BP-PID control, the lateral levelling time is 3.64 s, while under the QBP-PID control, the lateral levelling time is reduced to 2.98 s. Compared to the BP-PID and PID, the lateral levelling time is reduced by 18.13% and 27.66%, respectively.

(2) At a longitudinal tilt angle of 20°, the longitudinal levelling time under the PID control is 4.59 s, under the BP-PID control, the longitudinal levelling time is 4.14 s, whereas under the QBP-PID control, it decreases to 3.41 s. Compared to BP-PID and PID, the longitudinal levelling time is decreased by 17.63% and 31.6% respectively.

The QBP-PID omnidirectional rapid levelling control strategy proposed in this paper significantly reduces the levelling time for tractor seats in hilly and mountainous terrain. It effectively enhances driver comfort, alleviates operational fatigue, and provides an effective intelligent control solution for improving field operation efficiency and safety. However, certain limitations exist: the oil supply system was appropriately simplified during modelling; current simulations only address initial tilt angles of 15° laterally and 20° longitudinally. Future work will involve a thorough analysis of the impact of the oil supply system on levelling performance, further testing under continuously varying dynamic composite conditions, and consideration of hardware-in-the-loop simulation experiments to comprehensively validate the levelling system's capabilities.

ACKNOWLEDGMENTS

The authors thank the Henan Province K&D Project (251111111400, 231111112600), the Open Fund of State Key Laboratory of Mechanical Transmission for Advanced Equipment (SKLMT-MSKFKT-202506), the Postdoctoral Research Project of Henan Province (HN2026073), the Henan Provincial Natural Science Foundation Project (242300420369), the National Key R&D Program of China (2022YFD2001200), the Opening Foundation of Key Laboratory of Advanced Manufacture Technology for Automobile Parts, Ministry of Education (2024KLMT03), and the Heluo Youth Talent Support Program (2025HLTJ38).

REFERENCES

[1] Ingalls. M. L, "Mountain Agriculture: Opportunities for Harnessing Zero Hunger in Asia. Edited by Li Xuan, Mahmoud El Solh, and Kadambot H. M. Siddique," *Mountain Research and Development*, vol. 40, no. 9, pp. M2, 2020, doi: 10.1659/mrd.Mm257.1.

[2] B. Tong, P. Hu, and Y. Lian, "Analysis of Agricultural Mechanisation Development in Hilly and Mountainous Regions," *Hebei Agricultural Machinery*, no. 08, pp. 94-96, 2025, doi: 10.15989/j.cnki.hbnjzzs.2025.08.046.

[3] L. Zhao, G. Liu, Z. Lu, Y. Xiao, J. Nie, L. Yang, Z. Zhou, L. Chen, and H. Wang, "A new framework for delineating farmland consolidation priority areas for promoting agricultural mechanization in hilly and mountainous areas," *Computers and Electronics in Agriculture*, vol. 218, pp. 108681-, 2024, doi: 10.1016/j.Compag.2024.108681.

[4] G. Xue, J. Peng, H. Shen, G. Wang, W. Zheng, S. Huang, Z. Huan, L. Hu, and W. Ding, "Research Status and Prospects of Automatic Levelling Technology for Orchard Machinery," *Sustainability*, vol. 17, no. 12, pp. 5297, 2025, doi: 10.3390/su17125297.

[5] I. Ahmadi, "Dynamics of tractor lateral overturn on slopes under the influence of position disturbances (model development)," *Journal of Terramechanics*, vol. 48, no. 5, pp. 339-346, 2011, doi: 10.1016/j.jterra.2011.07.001.

[6] W. Qi, Y. Li, J. Tao, C. Qin, C. Liu, and K. Zhong, "Design and Experiment of Active Attitude Adjustment System for Hilly Area Tractors," *Trans. Chin. Soc. Agric. Mach*, vol. 50, no. 07, pp. 381-388, 2019, doi: 10.6041/j.issn.1000-1298.2019.07.042.

[7] G. Pan, F. Yang, J. Sun, and Z. Liu, "Analysis and Test of Obstacle Negotiation Performance of Small Hillside Crawler Tractor during Climbing Process," *Trans. Chin. Soc. Agric. Mach*, vol. 51, no. 09, pp. 374-383, 2020, doi: 10.6041/j.issn.1000-1298.2020.09.043.

[8] X. Mu, F. Yang, L. Duan, Z. Liu, Z. Song, Z. Li, and S. Guan, "Current status and development trends in key technologies for tractor levelling and rollover prevention in hilly and mountainous terrain," *SMART AGRICULTURE*, vol. 6, no. 03, pp. 1-16, 2024, doi: 10.12133/j.smartag.SA202312015.

[9] J. Sun, G. Chu, G. Pan, C. Meng, Z. Liu, and F. Yang, "Design and Performance Test of Remote control Omnidirectional Levelling Hillside Crawler Tractor," *Trans. Chin. Soc. Agric. Mach*, vol. 52, no. 05, pp. 358-369, 2021, doi: 10.6041/j.issn.1000-1298.2021.05.040.

[10] Q. Huang, M. Gao, Y. Wei, J. Zhang, and X. Jin, "Research on the Impact of Lumbar Support on Tractor Operators' Ride Comfort Considering Body Pressure Distribution and Subjective Assessment," *Agriculture*, vol. 15, no. 4, pp. 358-369, 2025, doi: 10.3390/agriculture15040410.

[11] X. Wei, Y. Li, J. Chen, S. Song, J. Gu, Z. Zuo, and J. Ni, "System integration of working process intelligent monitoring and controlling devices for combine harvester," *Transactions of the Chinese Society of Agricultural Engineering*, vol. 25, no. 1, pp. 56-60, 2009, doi: 10.3969/j.issn.1002-6819.2009.z2.011.

[12] X. Mou, Q. Luo, G. Ma, F. Wan, C. He, Y. Yue, Y. Yue, and X. Huang, "Simulation analysis and testing of tracked universal chassis passability in hilly mountainous orchards," *Agriculture*, vol. 13, no. 7, pp. 1458, 2025, doi: 10.3390/agriculture13071458.

[13] R.D. Haun, and H.J. Trefz, "MOWER DECK LEVELLING SYSTEM," U.S. Patent 14255573, Oct. 22, 2015.

[14] K.W. Hoehn, and W.L. Tompson, "Remotely adjustable disk levelling system," U.S. Patent 4809786A, Mar. 7, 1989.

[15] Leonard KE, and Woody VO, "Automatic levelling system," U.S. Patent 6106402, Aug. 22, 2000.

[16] P. Liu, C. Wang, H. Li, M. zhang, W. Wei, and S. Zhang, "Terrain Adaptive and Dynamic Levelling Agricultural Chassis for Hilly Area," *Trans. Chin. Soc. Agric. Mach*, vol. 49, no. 2, pp. 74-81, 2018, doi: 10.6041/j.issn.1000-1298.2018.02.010.

[17] P. Liu, F. Peng, H. Li, Z. Wang, W. Wei, and J. Zhao, "Design and Experiment of Adaptive Levelling Chassis for Hilly Area," *Trans. Chin. Soc. Agric. Mach*, vol. 48, no. 12, pp. 42-47, 2017, doi: 10.6041/j.issn.1000-1298.2017.12.005.

[18] J. Sun, C. Meng, Y. Zhang, G. Chu, Y. Zhang, F. Yang, and Z. Liu, "Design and physical model experiment of an attitude adjustment device for a crawler tractor in hilly and mountainous regions," *Information Processing in Agriculture*, vol. 7, no. 3, pp. 466-478, 2020, doi: 10.1016/j.inpa.2020.02.004.

[19] Y. Tang, "Research on automatic levelling systems for agricultural machinery driver Seat," M.E. thesis, Northwest A&F University, China, 2010.

[20] J. Su, P. Zhao, Q. Gao, G. Lu, D. Pan, Y. Luo, H. Xiang, J. Zeng, P. Xu, and Z. Mi, "A seat levelling device," C.N. Patent 216993989U, Jul. 19, 2022.

[21] Y. Yang, S. Cheng, J. Qi, G. Zhang, Q. Ma, and L. Chen, "Design and Test of Automatic Levelling System for Agricultural Machinery Seat Based on Ergonomics," *Trans. Chin. Soc. Agric. Mach*, vol. 53, no. 06, pp. 434-442, 2022, doi: 10.6041/j.issn.1000-1298.2022.06.046.

[22] H. Zhou, L. Hu, X. Luo, R. Zhao, Y. Xu, and W. Yang, "Design and Experiment on Auto Levelling System of Rotary Tiller," *Trans. Chin. Soc. Agric. Mach*, vol. 57, no. S1, pp. 117-123, 2016, doi: 10.6041/j.issn.1000-1298.2022.06.046.

[23] H. Yang, "Research on an automatic levelling control system for tractor chassis in hilly terrain based on Fuzzy PID control," M.E. thesis, Sichuan Agricultural University, China, 2021.

[24] W. Qi, "Research on active attitude control system for hill-climbing tractors," M.E. thesis, Shanghai Jiao Tong University, China, 2020.

[25] J. Zhang, Y. Li, W. Qi, C. Liu, F. Yang, and Z. Li, "Synchronous Control System of Tractor Attitude in Hills and Mountains Based on Neural Network PID," *Trans. Chin. Soc. Agric. Mach*, vol. 51, no. 12, pp. 356-366, 2020, doi: 10.6041/j.issn.1000-1298.2020.12.039.

[26] Z. Wang, "Research on electromechanical automatic levelling systems for construction vehicles," M.E. thesis, Shenyang University of Technology, China, 2022.

[27] S. T., S.S. Kanth, and S. K., "Reinforcement learning based adaptive PID controller design for control of linear/nonlinear unstable processes," *Applied Soft Computing Journal*, vol. 128, pp. 109450, 2022, doi: 10.1016/j.Asoc.2022.109450.

[28] S.A. Fayaz, S. Jahangeer Sidiq, M. Zaman, and M.A. Butt, "Machine learning: An introduction to reinforcement learning," *Machine Learning and Data Science: Fundamentals and Applications*, pp. 1-22, 2022, doi: 10.1002/9781119776499.ch1.

[29] V. Mathukumalli, "A tutorial introduction to reinforcement learning," *SICE Journal of Control, Measurement, and System Integration*, vol. 16, no. 1, pp. 172-191, 2023, doi: 10.1080/18824889.2023.2196033.

[30] R. Li, Y. Zhang, Z. Feng, J. Xu, X. Wu, M. Liu, Y. Xia, Q. Sun, and W. Yuan, "Review of the Progress of Energy Saving of Hydraulic Control Systems," *Processes*, vol. 11, no. 12, pp. 3304, 2023, doi: 10.3390/pr11123304.

[31] R. Li, W. Yuan, X. Ding, J. Xu, Q. Sun, and Y. Zhang, "Review of Research and Development of Hydraulic Synchronous Control System," *Processes*, vol. 11, no. 4, pp. 981, 2023, doi: 10.3390/pr11040981.

[32] R. Alexander, Z. Alexander, and P. Alexey, "Modeling and calculation of the technological process of testing piston hydraulic cylinders with energy recovery," in *E3S Web of Conferences*, 2023, pp. 01071, doi: 10.1051/e3sconf/202338101071.

[33] W. Cheng, "Mathematical Modeling and Experimental Study of Deflector Electro-hydraulic Servo Valve," M.E. thesis, Nanjing University of Aeronautics and Astronautics, China, 2023.

[34] Z. Luo, "Research on output speed control of tractor hydraulic mechanical continuously variable transmissions," M.E. thesis, Henan University of Science and Technology, China, 2024.

[35] Y. Jiang, Z. Sun, R. Wang, R. Ding, and Q. Ye, "Design and control of a new omnidirectional levelling system for hilly crawler work machines," *Computers and Electronics in Agriculture*, vol. 218, pp. 108661-, 2024, doi: 10.1016/j.Compag.2024.108661.

[36] W. Sun, H. Liu, R. Wang, T. Fu, J. Lv, and F. Wang, "Design and Experiment of PID Control Variable Application System Based on Neural Network Tuning," *Trans. Chin. Soc. Agric. Mach*, vol. 51, no. 12, pp. 55-64+94, 2020, doi: 10.6041/j.issn.1000-1298.2020.12.006.

[37] H. Wang, T. Wang, H. Hu, and X. Lu, "PID speed control of BLDCM based on Q-learning optimised BP Neural Network," *Journal of Jilin University (Engineering Edition)*, vol. 51, no. 06, pp. 2280-2286, 2021, doi: 10.13229/j.cnki.jdxbgxb20200580.